

# Investigation upon the performance of piezoelectric energy harvester with flexible extensions

Maoying Zhou, Weiting Liu

## 1. Model Description

We seek to investigate the influence of a flexible extension upon the overall performance of a classic piezoelectric cantilever beam energy harvester. In our problem, the energy harvester is comprised of two parts: the primary beam part and the beam extension part, as shown in Figure 1.

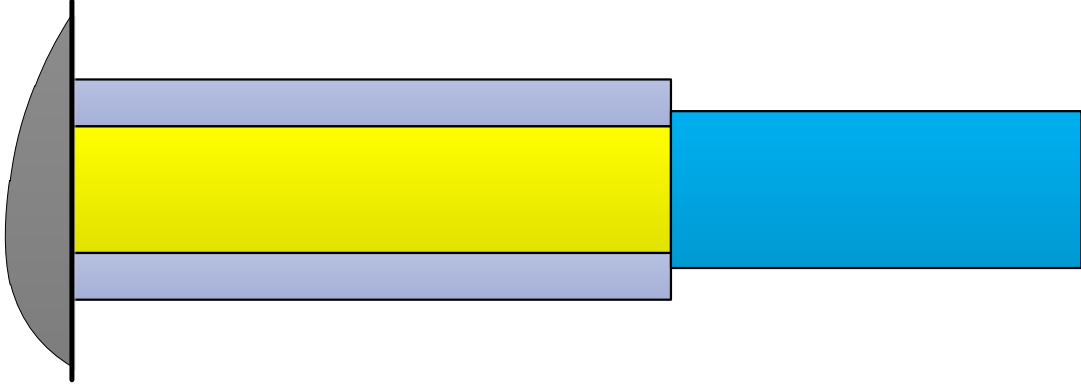


Figure 1: Schematic configuration of the piezoelectric energy harvester with flexible extension.

Following the classical analyzing process of piezoelectric bimorph cantilever beams [1, 2], we can simply list the following dimensional equations for the piezoelectric primary beam part as:

$$\begin{cases} M_p(x_1, t) = B_p \frac{\partial^2 w_1(x_1, t)}{\partial x_1^2} - e_p V_p(t) \\ q_p(x_1, t) = e_p \frac{\partial^2 w_1(x_1, t)}{\partial x_1^2} + \epsilon_p V_p(t), \end{cases} \quad (1)$$

where where  $M_p(x_1, t)$  is the moment at cross section of  $x_1$  and  $q_p(x_1, t)$  is the corresponding line charge density on the electrode.  $w_1(x_1, t)$  is the displacement function of the primary beam part with  $0 \leq x_1 \leq l_p$  and  $V_p(t)$  is the voltage across the electrodes. The corresponding coefficients  $B_p$ ,  $e_p$ , and  $\epsilon_p$  are defined as

$$B_p = \frac{2}{3}b \{E_s h_s^3 + c_{11}^E [(h_s + h_p)^3 - h_s^3]\}, \quad e_p = b e_{31} \left(h_s + \frac{1}{2}h_p\right), \quad \epsilon_p = \frac{b \epsilon_{33}^S}{2h_p} \quad (2)$$

in which  $c_{11}^E$  and  $E_s$  are the elastic constants of the piezoelectric layer and the structure layer, respectively,  $e_{31}$  is the piezoelectric charge constant of the piezoelectric layer,  $\epsilon_{33}^S$  is the dielectric constant of the piezoelectric layer,  $h_s$  and  $h_p$  are the half structure layer thickness and piezoelectric layer thickness, respectively,  $l_p$  is the length of the primary beam part, and  $b$  is the width of the primary beam part.

In terms of the mechanical balance, the equation of a piezoelectric beam can be established using the Euler-Bernoulli assumptions as follows

$$B_p \frac{\partial^4 w_1(x_1, t)}{\partial x_1^4} + m_p \frac{\partial^2 w_1(x_1, t)}{\partial t^2} = 0 \quad (3)$$

where  $m_p = 2b(\rho_s h_s + \rho_p h_p)$  is the line mass density of the primary beam part with  $\rho_s$  and  $\rho_p$  being the volumetric density of the structure layer and the piezoelectric layer, respectively. In turn, principally the piezoelectric energy harvester can be regarded as a current source. So we need to know the charge accumulated on the electrode  $Q_p(t)$ , which is calculated as

$$Q_p(t) = \int_0^{l_p} q_p(t) dx_1 = e_p \left[ \frac{\partial w_1(x_1, t)}{\partial x_1} \right] \Big|_0^{l_p} + C_p V_p(t) \quad (4)$$

where  $C_p = \epsilon_p l_p$  is the inherent capacitance of the piezoelectric layer. According to the Kirchhoff's law, the electric equilibrium equation is

$$\frac{dQ_p(t)}{dt} + \frac{V_p(t)}{R_l} = 0 \quad (5)$$

where  $R_l$  is the externally connected resistive load.

When it comes to the beam extension part ( $0 \leq x_2 \leq l_e$ ), the governing equations are

$$B_e \frac{\partial^4 w_2(x_2, t)}{\partial x_2^4} + m_e \frac{\partial^2 w_2(x_2, t)}{\partial t^2} = 0 \quad (6)$$

where  $w_2(x_2, t)$  is the displacement of the extension beam at position  $0 \leq x_2 \leq l_e$ ,  $B_e = \frac{2}{3}bh_e^3$  is the equivalent bending stiffness of the extension beam,  $m_e = \rho_e h_e$  is the line mass density of the extension beam,  $\rho_e$  is the volumetric mass density of the extension beam,  $h_e$  is the half thickness of the extension beam, and  $l_e$  is the length of the extension beam. As a result, the defining relations for the cross section moment  $M_e(x_2, t)$  at the position  $x_2$  is

$$M_e(x_2, t) = B_e \frac{\partial^2 w_2(x_2, t)}{\partial x_2^2}. \quad (7)$$

The related boundary conditions are listed as follows. When  $x_1 = 0$  at the fixed end of the primary beam,

$$w_1(0, t) = w_b(t), \quad w_1'(0, t) = 0, \quad (8)$$

where  $w_b(t)$  is the base excitation displacement function. Usually we use a harmonic vibration in the experiment where  $w_b(t) = Re \{ \xi_b e^{j\sigma t} \}$  with  $\sigma$  being the angular frequency of the base excitation signal and  $j = \sqrt{-1}$  being the imaginary unit. To be more accurate, the amplitude  $\xi_b$  is generally set to be a real constant designated by the controller. At the connection point of the primary beam and the beam extension where  $x_1 = l_p$  and  $x_2 = 0$ ,

$$\left\{ \begin{array}{l} w_1(l_p, t) = w_2(0, t) \\ \frac{\partial w_1(l_p, t)}{\partial x_1} = \frac{\partial w_2(0, t)}{\partial x_2} \\ B_p \frac{\partial^2 w_1(l_p, t)}{\partial x_1^2} - e_p V_p(t) = B_e \frac{\partial^2 w_2(0, t)}{\partial x_2^2} \\ B_p \frac{\partial^3 w_1(l_p, t)}{\partial x_1^3} = B_e \frac{\partial^3 w_2(0, t)}{\partial x_2^3} \end{array} \right. , \quad (9)$$

and at the free end of the beam extension where  $x_2 = l_e$ , we have

$$\frac{\partial^2 w_2(l_e, t)}{\partial x_2^2} = 0, \quad \frac{\partial^3 w_2(l_e, t)}{\partial x_2^3} = 0 \quad (10)$$

### 1.1. Harmonic Balance Analysis

Generally in the literature [1, 2], mode decomposition method or finite element method are used to solve the above described equations. Here in this contribution, as we are interested in the steady state response of the piezoelectric energy harvester, and the above described system are linear, harmonic balance method is used. Hence, as a result of the base excitation  $w_b(t) = Re \{ \xi_b e^{j\sigma t} \}$ , we can set the steady state response of the displacements  $w_1(x_1, t)$  and  $w_2(x_2, t)$  of the primary beam and the beam extension respectively as

$$w_1(x_1, t) = \tilde{w}_1(x_1) e^{j\sigma t}, \quad w_2(x_2, t) = \tilde{w}_2(x_2) e^{j\sigma t}, \quad (11)$$

the steady state voltage response  $V_p(t)$  and charge accumulation  $Q_p(t)$  as

$$V_p(t) = \tilde{V}_p e^{j\sigma t}, \quad Q_p(t) = \tilde{Q}_p e^{j\sigma t}, \quad (12)$$

and the cross section moment  $M_p(x_1, t)$  and  $M_e(x_2, t)$  described as

$$M_p(x_1, t) = \tilde{M}_p(x_1) e^{j\sigma t}, \quad M_e(x_2, t) = \tilde{M}_e(x_2) e^{j\sigma t}. \quad (13)$$

As a result, the system of equations for the piezoelectric energy harvester can be summarized as

$$\begin{cases} B_p \frac{\partial^4 \tilde{w}_1(x_1)}{\partial x_1^4} - m_p \sigma^2 \tilde{w}_1(x_1) = 0 \\ B_e \frac{\partial^4 \tilde{w}_2(x_2)}{\partial x_2^4} - m_e \sigma^2 \tilde{w}_2(x_2) = 0, \\ j\sigma \tilde{Q}_p + \frac{\tilde{V}_p}{R_l} = 0 \end{cases} \quad (14)$$

$$\begin{cases} \tilde{M}_p(x_1) = B_p \frac{\partial^2 \tilde{w}_1(x_1)}{\partial x_1^2} - e_p \tilde{V}_p \\ \tilde{Q}_p = e_p \left[ \frac{\partial \tilde{w}_1(x_1)}{\partial x_1} \right] \Big|_0^{l_p} + C_p \tilde{V}_p, \\ \tilde{M}_e(x_2) = B_e \frac{\partial^2 \tilde{w}_2(x_2)}{\partial x_2^2} \end{cases} \quad (15)$$

and the boundary conditions become

$$\begin{cases} \tilde{w}_1(0) = \xi_b, \quad \frac{\partial \tilde{w}_1}{\partial x_1}(0) = 0 \\ w_1(l_p, t) = w_2(0, t), \quad \frac{\partial \tilde{w}_1(l_p)}{\partial x_1} = \frac{\partial \tilde{w}_2(0)}{\partial x_2} \\ B_p \frac{\partial^2 \tilde{w}_1(l_p)}{\partial x_1^2} - e_p \tilde{V}_p = B_e \frac{\partial^2 \tilde{w}_2(0)}{\partial x_2^2}, \quad B_p \frac{\partial^3 \tilde{w}_1(l_p)}{\partial x_1^3} = B_e \frac{\partial^3 \tilde{w}_2(0)}{\partial x_2^3} \\ \frac{\partial^2 \tilde{w}_2(l_e)}{\partial x_2^2} = 0, \quad \frac{\partial^3 \tilde{w}_2(l_e)}{\partial x_2^3} = 0 \end{cases} \quad (16)$$

From the equations (14), (15), and (16), we can eliminate the electrical quantities  $\tilde{Q}_p$  and  $\tilde{V}_p$  by incorporating them into the boundary conditions. Actually, from equations (14) and (15), we have

$$\tilde{V}_p = \frac{j\sigma R_l e_p}{j\sigma R_l C_p + 1} \left[ \frac{\partial \tilde{w}_1(x_1)}{\partial x_1} \right] \Big|_0^{l_p} \quad (17)$$

which can actually be used to eliminate the term  $\tilde{V}_p$  in the boundary conditions (16). In the end, we can simplify the problem as a combination of the governing equations

$$\begin{cases} B_p \frac{\partial^4 \tilde{w}_1(x_1)}{\partial x_1^4} - m_p \sigma^2 \tilde{w}_1(x_1) = 0 \\ B_e \frac{\partial^4 \tilde{w}_2(x_2)}{\partial x_2^4} - m_e \sigma^2 \tilde{w}_2(x_2) = 0 \end{cases} \quad (18)$$

and the boundary conditions

$$\left\{ \begin{array}{ll} \tilde{w}_1(0) = \xi_b, & \frac{\partial \tilde{w}_1}{\partial x_1}(0) = 0 \\ \tilde{w}_1(l_p) = \tilde{w}_2(0), & \frac{\partial \tilde{w}_1(l_p)}{\partial x_1} = \frac{\partial \tilde{w}_2(0)}{\partial x_2} \\ B_p \frac{\partial^2 \tilde{w}_1(l_p)}{\partial x_1^2} + \frac{j\sigma R_l e_p^2}{j\sigma R_l C_p + 1} \frac{\partial \tilde{w}_1(l_p)}{\partial x_1} = B_e \frac{\partial^2 \tilde{w}_2(0)}{\partial x_2^2}, & B_p \frac{\partial^3 \tilde{w}_1(l_p)}{\partial x_1^3} = B_e \frac{\partial^3 \tilde{w}_2(0)}{\partial x_2^3} \\ \frac{\partial^2 \tilde{w}_2(l_e)}{\partial x_2^2} = 0, & \frac{\partial^3 \tilde{w}_2(l_e)}{\partial x_2^3} = 0 \end{array} \right. \quad (19)$$

which actually manifests as a boundary value problem.

## 2. Dimensionless Problem

Using the following dimensionless group

$$\tilde{w}_1, \tilde{w}_2 \sim \xi_b, \quad \tilde{x}_1 \sim l_p, \quad \tilde{x}_2 \sim l_e \quad (20)$$

we can nondimensionalize the above formulated boundary value problem with respect to the following variables:

$$\tilde{w}_1 = \xi_b u_1, \quad \tilde{w}_2 = \xi_b u_2, \quad \tilde{x}_1 = l_p x, \quad \tilde{x}_2 = l_e x. \quad (21)$$

Note that here we use one independent space variable  $x$  to nondimensionalize two previously used variables  $x_1$  and  $x_2$ . This comes from the fact that the variables  $x_1$  and  $x_2$  are not coupled with each other in the sense that the primary beam and the extension beam do not overlap each other except for their joint point where  $x_1 = l_p$  and  $x_2 = 0$ . Thus the two variables do not occur in the equations simultaneously except for the boundary conditions. As for the boundary conditions, the change of variables does not affect the values of the equations. Therefore, the two parts of the piezoelectric energy harvester beam are in fact independent of each other except for the joining point. In one word, the equation (21) does not change the problem in essence.

Hence, the above boundary value problem is further changed into the combination of the governing equations

$$\begin{cases} \frac{B_p}{l_p^4} u_1'''' - m_p \sigma^2 u_1 = 0 \\ \frac{B_e}{l_e^4} u_2'''' - m_e \sigma^2 u_2 = 0 \end{cases} \quad (22)$$

and the boundary conditions

$$\left\{ \begin{array}{l} u_1(0) = 1, \quad u_1'(0) = 0 \\ u_1(1) = u_2(0), \quad \frac{1}{l_p} u_1'(1) = \frac{1}{l_e} u_2'(0) \\ \frac{B_p}{l_p^2} u_1''(1) + \frac{j\sigma R_l e_p^2}{j\sigma R_l C_p + 1} \frac{1}{l_p} u_1'(1) = \frac{B_e}{l_e^2} u_2''(0), \quad \frac{B_p}{l_p^3} u_1'''(1) = \frac{B_e}{l_e^3} u_2'''(0) \\ u_2''(1) = 0, \quad u_2'''(1) = 0 \end{array} \right. \quad (23)$$

in which the prime means the derivative with respect to  $x$ . The equations can again be organized in a more compact form

$$\left\{ \begin{array}{l} u_1'''' - \nu^2 u_1 = 0 \\ u_2'''' - \nu^2 \lambda_m \lambda_l^4 / \lambda_B u_2 = 0 \end{array} \right. \quad (24)$$

and the boundary conditions

$$\left\{ \begin{array}{l} u_1(0) = 1, \quad u_1'(0) = 0 \\ u_1(1) = u_2(0), \quad \lambda_l u_1'(1) = u_2'(0) \\ u_1''(1) + \frac{j\nu\beta}{j\nu\beta + 1} \alpha^2 u_1'(1) = \lambda_B / \lambda_l^2 u_2''(0), \quad u_1'''(1) = \lambda_B / \lambda_l^3 u_2'''(0) \\ u_2''(1) = 0, \quad u_2'''(1) = 0 \end{array} \right. \quad (25)$$

where

$$\nu = \sigma \sqrt{\frac{m_p l_p^4}{B_p}}, \quad \lambda_B = \frac{B_e}{B_p}, \quad \lambda_m = \frac{m_e}{m_p}, \quad \lambda_l = \frac{l_e}{l_p} \quad (26)$$

$$\beta = R_l C_p \sqrt{\frac{B_p}{m_p l_p^4}}, \quad \alpha = e_p \sqrt{\frac{l_p}{C_p B_p}} \quad (27)$$

The system (24) and (25) is a two-point boundary value problem. The problem can readily be solved by a Chebyshev collocation method using the MATLAB package *Chebfun* [3].

### 3. Influence of extension part upon energy harvester performance

The basic geometry and material properties of the materials used in the proposed piezoelectric energy harvester with flexible extensions are summarized in Table 1. Note that some of the parameters, like length  $l_e$ , Young's modulus  $Y_e$ , and volumetric density  $\rho_e$  of the beam extension, are actually changing across different simulations. In the simulation, base excitation frequency  $fr$  and external load resistance  $R_l$ , which change the dimensionless values of  $\nu$  and  $\beta$ , respectively, are of critical importance in the sense that these two parameters reflect the influence of vibration source frequency spectrum and external load circuit. For every set of parameter values, we set the base excitation frequency  $fr$  to change from 1  $Hz$  to 100  $Hz$ , which covers the usual frequency range of natural vibration sources, and set the load resistance  $R_l$  to change from 1  $\Omega$  to 10  $M\Omega$ , which is inspired by the Ref. [1] and takes into account the dielectric property of piezoelectric materials. Actually, when the load resistance  $R_l = 1 \Omega$ , the piezoelectric energy harvester is said to be in a short-circuit condition as the general equivalent resistance of the structure is much larger than  $R_l$ . On the other hand, when  $R_l = 10 M\Omega$ , the system is close to an open-circuit condition where no external load is connected to the output electrodes.

In the following, we will investigate the influences of length  $l_e$ , Young's modulus  $Y_e$ , and volumetric density  $\rho_e$  of the beam extension upon the performance of the piezoelectric energy harvester with flexible extensions separately.

Table 1: Geometric, material, and electromechanical parameters of the simulation for piezoelectric energy harvester with flexible extension

Parameter item	Parameter value
Length of the primary beam, $l_p$ (mm)	100
Width of the whole energy harvester, $b$ (mm)	20
Half thickness of the structure, $h_s$ (mm)	0.25
Thickness of the piezoelectric layer, $h_p$ (mm)	0.2
Young's modulus of the structure, $Y_s$ (Gpa)	100
Young's modulus of the piezoelectric layer, $Y_p$ (Gpa)	66
Mass density of the substructure, $\rho_s$ (kg/m <sup>3</sup> )	7165
Mass density of the piezoelectric layer, $\rho_p$ (kg/m <sup>3</sup> )	7800
piezoelectric constant, $d_{31}$ (pm/V)	-190
Permittivity, $\epsilon_{33}^S$ (nF/m)	15.93
Length of the beam extension, $l_e$ (mm)	30
Young's modulus of the beam extension, $Y_e$ (Gpa)	2.3
Mass density of the beam extension, $\rho_e$ (kg/m <sup>3</sup> )	1.38
Half thickness of the structure, $h_e$ (mm)	0.25

### 3.1. beam extension length $l_e$ or length ratio $\lambda_l$

The presence of the beam extension is firstly controlled by the beam extension length  $l_e$  or length ratio  $\lambda_l$ , equivalently. When  $\lambda_l = 0.0$ , no beam extension is attached the resultant energy harvester reduces to the classical piezoelectric energy harvesting bimorph. [1] In our research, this case is referred to as a reference. In the considered range of length ratio  $0 \leq \lambda_l \leq 1$ , the base excitation problem is solved with respect to different base excitation frequency  $fr$  and external load resistance  $R_l$ .

In the first place, we plot the resulting amplitude of output voltage  $V_p$  with respect to the length ratio of  $\lambda_l = 0, 0.2, 0.4, 0.6, 0.8, 1.0$  in Figure 2 and the corresponding amplitude of output power  $P_p$  in Figure 3.

According to Figure 2 and Figure 3, for given  $\lambda_B$  and  $\lambda_m$ , frequency response of the piezoelectric energy harvester in the interested frequency range (1 – 100 Hz) changes in accordance with the extension length  $l_e$  and thus the length ratio  $\lambda_l$ . When  $\lambda_l$  is relatively small, say  $\lambda_l = 0.1$  and  $\lambda_l = 0.2$  ( as shown in Figure 2(b)) in our case, the vibration of the whole beam is almost the same as that of the case where  $\lambda_l = 0.0$ . Only slight change of the resonant frequency of eigen mode (We call this mode  $L1$ ) is observed. Therefore the beam extension part is playing a negligible role in the motion of the primary beam part. As a result, energy harvesting performances of the proposed piezoelectric energy harvesters with flexible extensions are similar to that of a classic cantilever beam based piezoelectric energy harvester.

With the increase of the length ratio  $\lambda_l$ , say  $\lambda_l = 0.4, 0.6$ , or  $0.8$ , there begins to exist an extra resonant and anti-resonant mode in the considered frequency range, compared with that of the case where  $\lambda_l = 0.0$ . What's more, for the cases of  $\lambda_l = 0.4$  and  $0.6$ , the shift of the resonant frequency of mode  $L1$  is significant compared with the case of small  $\lambda_l$ . Meanwhile, when  $\lambda_l = 0.8$ , the frequency shift is again negligible.

With further increase of the length ratio to  $\lambda_l = 1.0$ , two extra resonant and anti-resonant modes occur in the considered frequency range and the frequency shift begins to be important.

In this view, the attachment of the flexible extension part may introduces extra vibration modes in the considered frequency range. Noting that typical piezoelectric energy harvesters rely on resonant modes to work, this will actually expands the bandwidth of the proposed piezoelectric energy harvester. On the other hand, the flexible extension also provides a way to tune the bandwidth of a piezoelectric energy harvester. The point to be noticed is the existence of anti-resonant modes. They correspond to low output voltage and output power, and to some degree narrows the bandwidth of the energy harvester. However, it is still not worse than an otherwise non-resonant vibration, as in both cases the

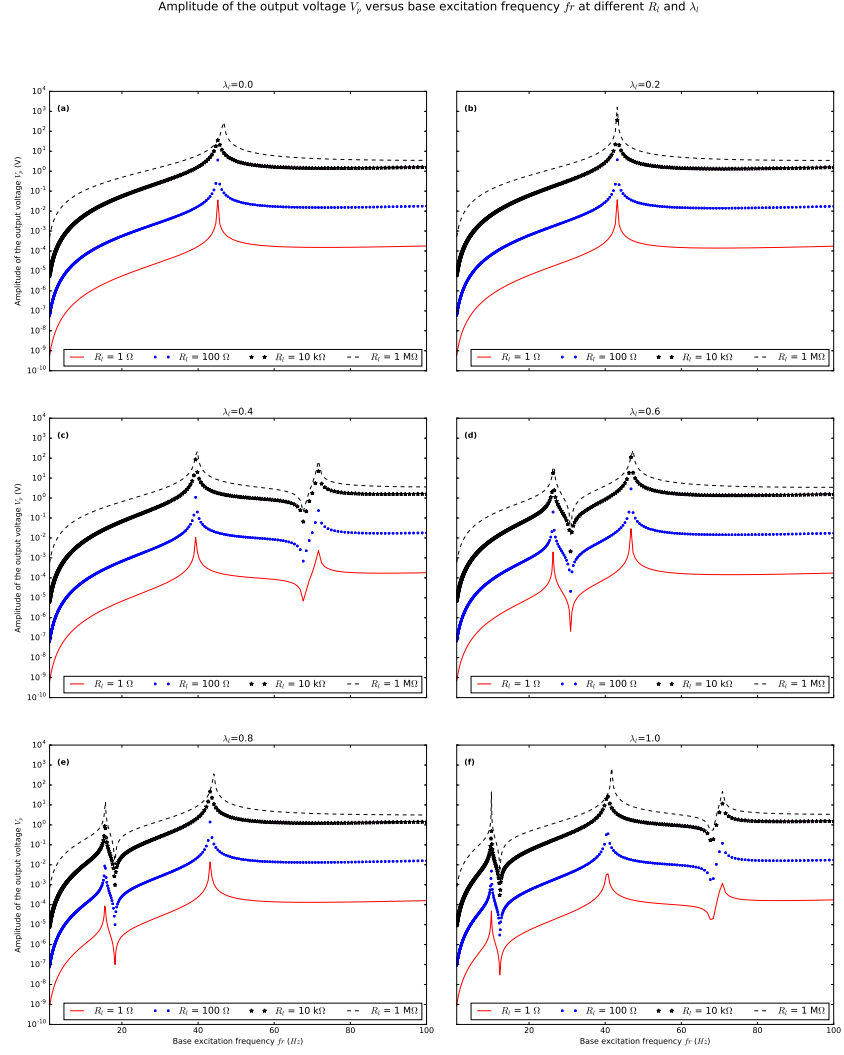


Figure 2: Output voltage  $V_p$  (amplitude) of the piezoelectric energy harvester with flexible extension versus length ratio  $\lambda_l$  at different frequency  $f$  and load resistance  $R_l$ .

electrical output of the piezoelectric energy harvester is unusable.

Amplitude of the output power  $P_p$  versus base excitation frequency  $f_r$  at different  $R_l$  and  $\lambda_l$

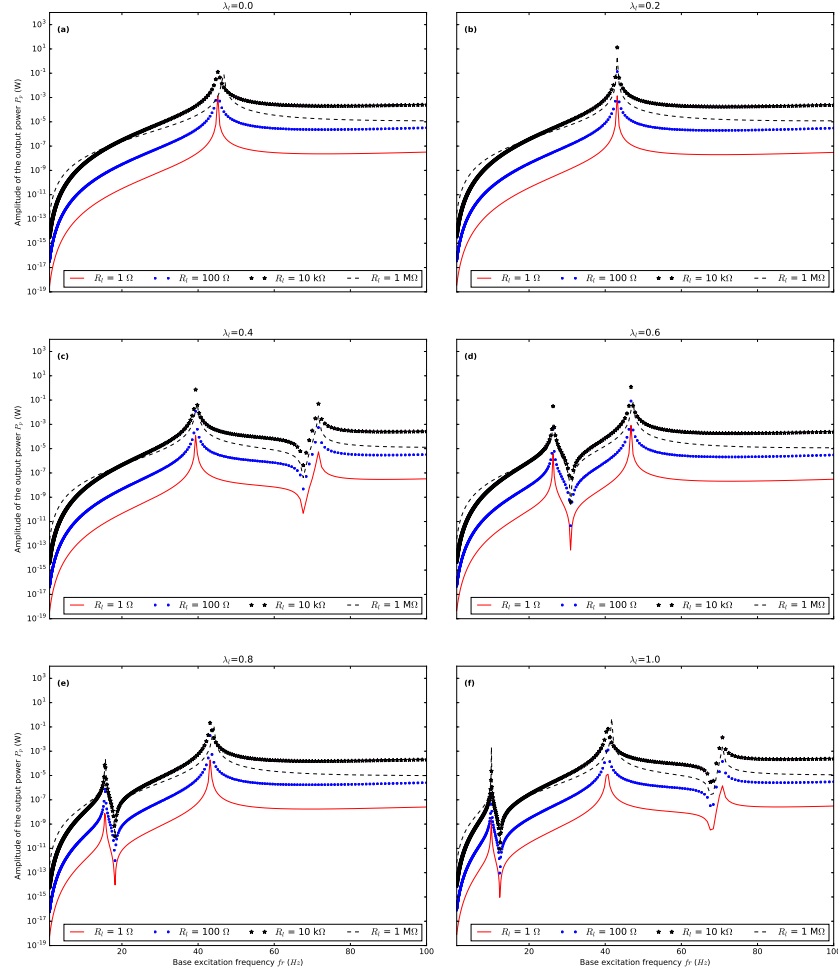


Figure 3: Output power  $P_p$  (amplitude) of the piezoelectric energy harvester with flexible extension versus length ratio  $\lambda_l$  at different frequency  $f$  and load resistance  $R_l$ .

In the second place, we compare the case where  $\lambda = 0.3$  and  $0.4$  with the reference case where  $\lambda = 0.0$  in terms of different externally connected resistance  $R_l$ . The resulting amplitude of output voltage  $V_p$  and output power  $P_p$  are shown in Figure 4. It is obvious that in the range of low  $R_l$ , a power law exists between the amplitudes of output voltage and power and the connected resistance  $R_l$ . For all the chosen frequency values  $f_r$ , the increase of  $R_l$  leads to an increase in  $V_p$ , and finally it is found that  $V_p$  approaches asymptotically to a limit value  $V_p^{lim}$ . This value actually corresponds to the open-circuit output voltage of the piezoelectric energy harvester. At the same time, the value of  $P_p$  exhibits an



obvious maximum at some values of  $R_l$  between  $10k\Omega$  and  $1M\Omega$ . And away from the maximum value, we see also a power law between the value of  $R_l$  and  $P_p$ . This indicates that an asymptotic analysis may help us to simplify the analysis of performance of piezoelectric energy harvesters. But this is out of the scope of our current contribution and will be covered in the future research.

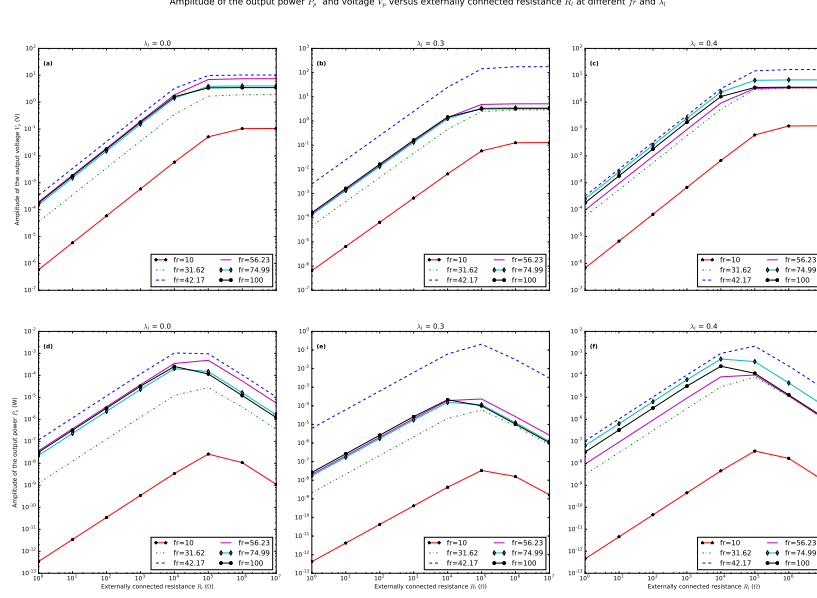


Figure 4: Output voltage  $V_p$  (amplitude) and output power  $P_p$  (amplitude) of the piezoelectric energy harvester with flexible extension versus bending stiffness ratio  $\lambda_l$  at different frequency  $f_r$  and load resistance  $R_l$ .

In the third place, at different values of  $f_r$  and  $R_l$ , we directly plot the amplitudes of  $V_p$  and  $P_p$  with respect to  $\lambda_l$ , which are shown in Figure 5 and Figure 5. It is shown from the figures that at given values of  $R_l$  and  $f_r$ , output performances of the proposed piezoelectric energy harvesters can be tuned by the parameter  $\lambda_l$ . For example, when  $f_r = 31.62 \text{ Hz}$  and  $R_l = 10 \text{ k}\Omega$ , a maximum peak around  $\lambda_l = 0.5$  is shown if we increase the values of  $\lambda_l$ . Compared with the case of no extension ( $\lambda_l = 0$ ), the amplitude of output voltage  $V_p$  is about 3 times larger, while the amplitude of output power  $P_p$  is about 3 times larger. This indicates that the addition of the flexible extension can substantially increase the output performance of a piezoelectric energy harvester. It should be noted that in case of large values of  $f_r$ , like  $f_r = 100 \text{ Hz}$ , the tuning performance of the flexible extension is no longer significant.

### 3.2. beam extension bending stiffness or bending stiffness ratio $\lambda_B$

It is easily seen from the diagram that the change of extension length  $l_e$  have a great influence on the frequency response of the piezoelectric energy harvester. At the given values of  $\lambda_B$  and  $\lambda_m$ , the contained vibration modes in the frequency range considered does change with respect to the length ratio  $\lambda_l$ . When  $\lambda_l$  is relatively small, which is below 0.3 in our case, no extra vibration modes can be found in the frequency range of  $1 - 100 \text{ Hz}$ . Hence the energy harvesting performances of the proposed energy harvesters are similar to that of a pure cantilever beam piezoelectric energy harvester. (note: it will be better if I can compare the resonant energy harvesting performance in this case) With further increase of the length ratio  $\lambda_l$ , there begins to exist an extra resonant and anti-resonant mode in the considered frequency range. In this view, the change of length ratio actually expands the bandwidth of the energy harvesting performances. Even when

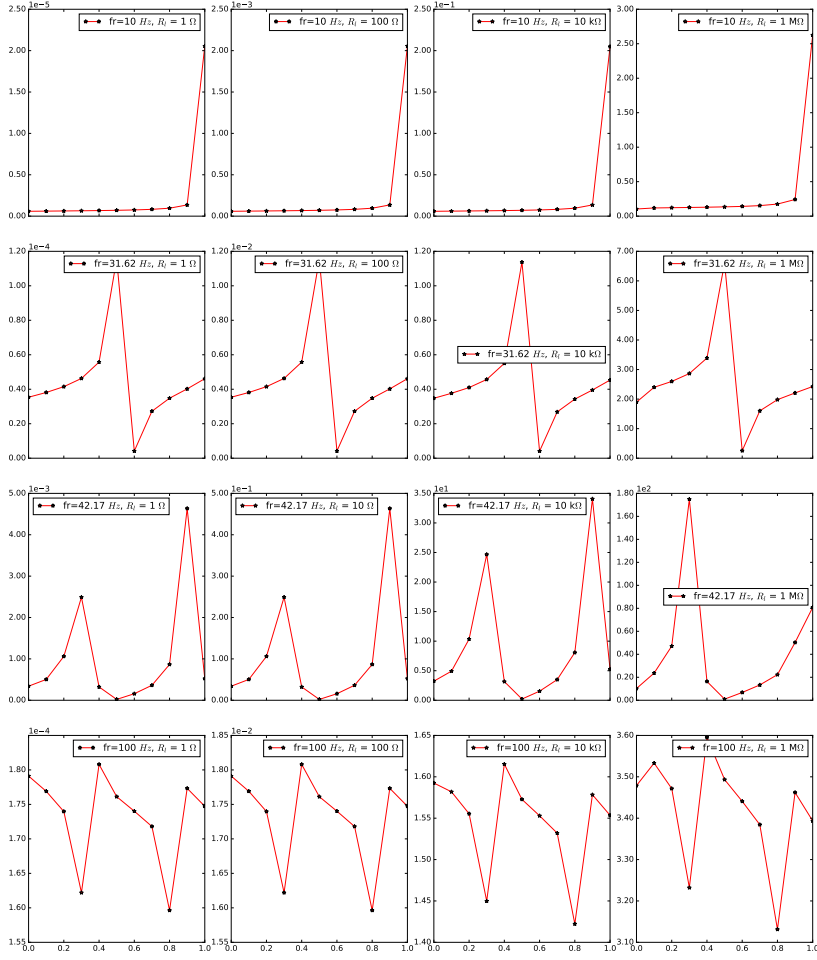


Figure 5: Output voltage  $V_p$  (amplitude) and output power  $P_p$  (amplitude) of the piezoelectric energy harvester with flexible extension versus bending stiffness ratio  $\lambda_l$  at different frequency  $f$  and load resistance  $R_l$ .

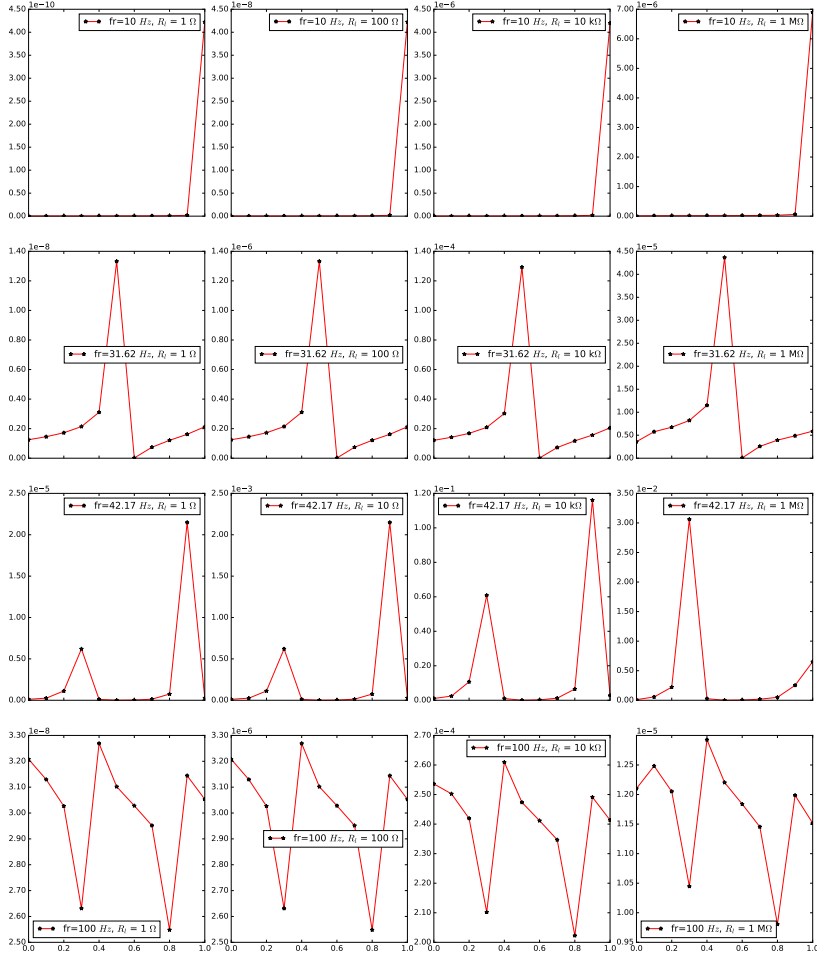


Figure 6: Output voltage  $V_p$  (amplitude) and output power  $P_p$  (amplitude) of the piezoelectric energy harvester with flexible extension versus bending stiffness ratio  $\lambda_l$  at different frequency  $f$  and load resistance  $R_l$ .

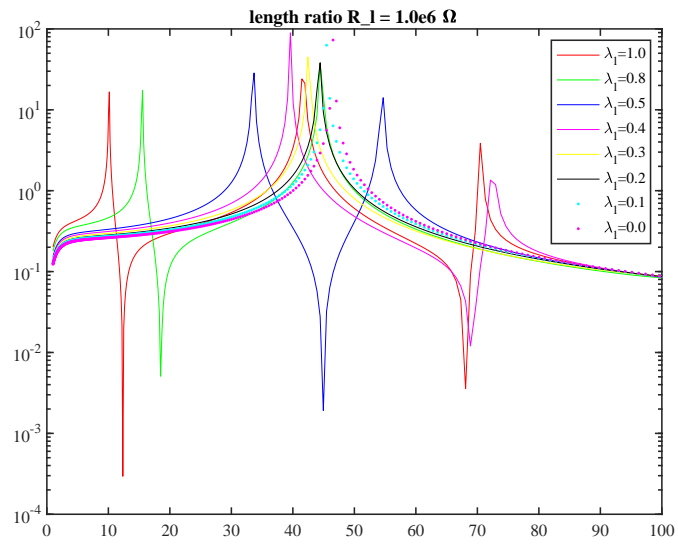


Figure 7: Output voltage  $V_p$  (amplitude) and output power  $P_p$  (amplitude) of the piezoelectric energy harvester with flexible extension versus bending stiffness ratio  $\lambda_l$  at different frequency  $f$  and load resistance  $R_l$ .

the length ratio  $\lambda_l = 1.0$ , three resonant modes are found in the frequency range. The point to be noticed is the existence of anti-resonant mode, which largely narrows the bandwidth of the energy harvester. This accompanying characteristic is to be further investigated in the following research.

### 3.3. beam extension line density or line density ratio $\lambda_m$

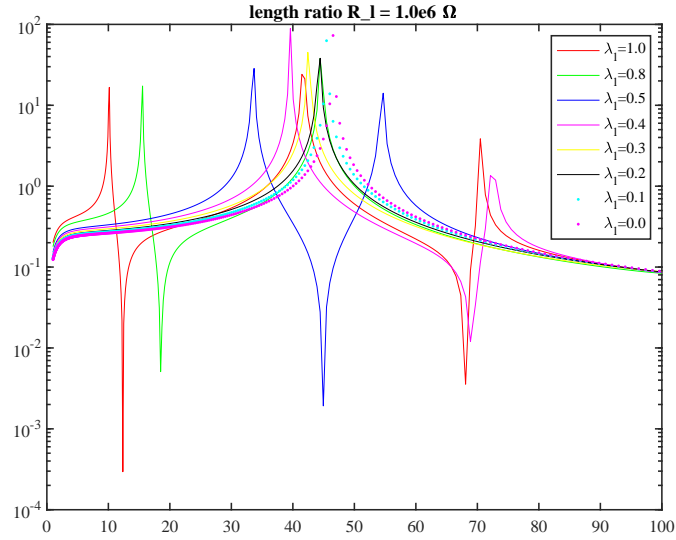


Figure 8: Output voltage  $V_p$  (amplitude) and output power  $P_p$  (amplitude) of the piezoelectric energy harvester with flexible extension versus line mass density ratio  $\lambda_m$  at different frequency  $f$  and load resistance  $R_l$ .

It is easily seen from the diagram that the change of extension length  $l_e$  have a great influence on the frequency response of the piezoelectric energy harvester. At the given values of  $\lambda_B$  and  $\lambda_m$ , the contained vibration modes in the frequency range considered does change with respect to the length ratio  $\lambda_l$ . When  $\lambda_l$  is relatively small, which is below 0.3 in our case, no extra vibration modes can be found in the frequency range of 1 – 100  $Hz$ . Hence the energy harvesting performances of the proposed energy harvesters are similar to that of a pure cantilever beam piezoelectric energy harvester. (note: it will be better if I can compare the resonant energy harvesting performance in this case) With further increase of the length ratio  $\lambda_l$ , there begins to exist an extra resonant and anti-resonant mode in the considered frequency range. In this view, the change of length ratio actually expands the bandwidth of the energy harvesting performances. Even when the length ratio  $\lambda_l = 1.0$ , three resonant modes are found in the frequency range. The point to be noticed is the existence of anti-resonant mode, which largely narrows the bandwidth of the energy harvester. This accompanying characteristic is to be further investigated in the following research.

#### 4. Discussion

#### 5. Conclusion

Here in this contribution, we investigate the method of flexible extension to tune the energy harvesting performance of piezoelectric cantilever energy harvester.

#### Reference

- [1] Erturk A, Inman DJ. An experimentally validated bimorph cantilever model for piezoelectric energy harvesting from base excitations. *Smart materials and structures*. 2009;18(2):025009.
- [2] Park CH. Dynamics modelling of beams with shunted piezoelectric elements. *Journal of Sound and vibration*. 2003;268(1):115–129.
- [3] Driscoll TA, Hale N, Trefethen LN. *Chebfun guide*. Pafnuty Publications, Oxford; 2014.